# Synchrotron Radiation Studies of Nuclear-Resonant Scattering in the Presence of Strong Electronic Charge Scattering

J. B. Hastings, D. P. Siddons, G. Faigel,[a] L. E. Berman, P. E. Haustein, and J. R. Grover
*Brookhaven National Laboratory, Upton, New York 11973*
(Received 31 July 1989)

The delayed nuclear-resonant Bragg scattering of synchrotron radiation at a strong allowed charge scattering peak in $\alpha$-$^{57}Fe_2O_3$ has been observed. The detailed time dependence has been measured and successfully interpreted theoretically. This result demonstrates that it is no longer necessary to extinguish crystallographically the normal charge scattering in synchrotron radiation studies of nuclear-resonant scattering.

PACS numbers: 76.80.+y, 07.85.+n, 25.20.Dc, 78.70.Ck

Synchrotron radiation (SR) has revolutionized x-ray studies over the last decade. One of the areas still at the frontier is inelastic x-ray scattering with energy resolutions in the sub-meV range. Conventional crystal monochromators are limited to resolving powers of several million due to extinction. Nuclear-resonant scattering has been suggested[1] as an alternative since it can provide monochromaticities which are controlled by the width of the resonance rather than the width of a Bragg reflection. In $^{57}Fe$ this width is $5\times10^{-9}$ eV. The possibility of attaining such high resolution has stimulated several studies of nuclear Bragg scattering of SR from nearly perfect crystals containing $^{57}Fe$. In particular, $Fe_2O_3$,[2-5] yttrium iron garnet (YIG),[6-8] and $FeBO_3$ (Ref. 9) have been investigated with respect to the temporal and polarization dependencies of the scattered radiation. In studies with each of these materials, the normal charge scattering was suppressed by choosing electronically forbidden, but nuclear allowed, Bragg peaks.

In this Letter we report the observation of nuclear-resonant scattering of SR at a Bragg peak for which the normal electronic charge scattering was not extinguished. The temporal dependence of the resonant signal was measured and is shown to agree well with theory. Previous observations of nuclear-resonant scattering at an electronically allowed Bragg peak have been made with a single line source.[10] Our ability to make such an observation using SR, however, relied critically on a narrow bandwidth ($\Delta E = 5$ meV), highly collimated excitation beam.[11] The significance of this observation lies in the removal of restrictions on sample crystallography (i.e., the use of antiferromagnets and ferrimagnets or other systems for which the normal charge scattering is extinguished), making the stimulation of low-lying nuclear excitations by SR a much more versatile and generally applicable technique.

The theory of nuclear Bragg scattering has been developed over the last three decades.[12-15] Following the notation of van Bürck *et al.*,[16] both the normal charge scattering and the resonant nuclear scattering can be included in the scattering amplitude for energies near resonance. The normal charge scattering amplitude is[16]

$$F^e_{ji} = -r_e\sum_v (f_{0v}+f'_v-if''_v)\exp(-M_v)\exp[i(\mathbf{k}_j-\mathbf{k}_i)\cdot\mathbf{r}_v]P^e_{ji}\,. \tag{1}$$

The sum is over the $v$ atoms of the unit cell; the position of each is denoted by $\mathbf{r}_v$. The index $i,j=0$ refers to the incident-beam direction and $i,j=1$ to the scattered-beam direction; $\mathbf{k}_0$ and $\mathbf{k}_1$ refer to the incident and scattered wave vectors, respectively. $r_e$ is the classical electron radius, $f_{0v}$ is the atomic form factor for normal charge scattering, and $f'_v$ and $f''_v$ are the anomalous dispersion corrections. $\exp(-M_v)$ is the Debye-Waller factor, and $\exp[i(\mathbf{k}_j-\mathbf{k}_i)\cdot\mathbf{r}_v]$ is a geometrical phase factor. $P^e_{ji}$ is a polarization factor, given by[16]

$$P^e_{ji} = \hat{\boldsymbol{\epsilon}}_j\cdot\hat{\boldsymbol{\epsilon}}_i\,, \tag{2}$$

where $\hat{\boldsymbol{\epsilon}}_0$ and $\hat{\boldsymbol{\epsilon}}_1$ are unit vectors directed along the electric fields of the incident and diffracted beams, respectively. It should be noted that the off-resonant magnetic x-ray scattering is not included since it is several orders of magnitude weaker than the normal charge scattering for our experimental conditions.

The nuclear-resonant scattering amplitude is given by[16]

$$F^{n(l)}_{ji} = -\left(\frac{3}{2k_{\rm vac}}\right)\sum_\rho\left(\frac{1}{2I_g+1}\right)\left(\frac{\eta}{1+\alpha}\right)\left(\frac{\Gamma/2}{(E-E_{0l})+i(\Gamma/2)}\right)$$
$$\times C_l^2(I_g,1,I_e;m_{gl},\Delta m_l)f_\rho(\mathbf{k}_j)f_\rho(\mathbf{k}_i)\exp[i(\mathbf{k}_j-\mathbf{k}_i)\cdot\mathbf{r}_\rho]P^{n(l)}_{ji}\,. \tag{3}$$


© 1989 The American Physical Society

Here the sum is over the $\rho$ resonant atoms in the unit cell. $E$ is the incident photon energy and $k_{vac}$ is the magnitude of the incident wave vector. $I_g$ and $I_e$ are the ground- and excited-state spins of the nucleus, respectively, $\eta$ is the abundance of the resonant nuclei, and $\alpha$ is the conversion coefficient. $E_{0l}$ denotes the energy of the $l$th multiplet level and $\Gamma$ its total width. $f_\rho(\mathbf{k}_j)$ and $f_\rho(\mathbf{k}_i)$ are the Lamb-Mössbauer temperature factors, $C_l$ is the Clebsch-Gordan coefficient for a given transition from $I_g$ to $I_e$, and $\Delta m_l$ is the corresponding change in the magnetic quantum number. $\exp[i(\mathbf{k}_j-\mathbf{k}_i)\cdot\mathbf{r}_\rho]$ is again a geometrical phase factor, and $P_{ji}^{n(l)}$ is a polarization factor, given by[16]

$$P_{ji}^{n(l)}=(\hat{\mathbf{h}}_j\cdot\hat{\mathbf{u}}_l)(\hat{\mathbf{h}}_i\cdot\hat{\mathbf{u}}_l)^*\,, \tag{4}$$

where $\hat{\mathbf{h}}_0$ and $\hat{\mathbf{h}}_1$ are unit vectors directed along the magnetic fields of the incident and diffracted beams, respectively, and $\hat{\mathbf{u}}_l$ is a unit vector equal to $\hat{\mathbf{u}}_z$, the quantization axis unit vector (which is parallel to the nuclear-spin vector), for $\Delta m=0$ transitions, and equal to $\mp(\hat{\mathbf{u}}_x \pm i\hat{\mathbf{u}}_y)/\sqrt{2}$ for $\Delta m=\pm 1$ transitions. Using these expressions in the dynamical theory of x-ray scattering, the response in the time domain of the Bragg scattering near the 14.4-keV nuclear resonance in $^{57}$Fe can be calculated for any Bragg reflection from $Fe_2O_3$.

The measurements were made at the Cornell High Energy Synchrotron Source (CHESS). The six-pole wiggler installed on the Cornell Electron Storage Ring (CESR) provided the radiation. Machine parameters were typically 35–60 mA of stored current at 5-GeV electron energy. The experimental arrangement[11] was similar to that used in our previous studies,[3-5] except for the use of a plastic-scintillator detector in place of an intrinsic Ge solid-state detector to provide the needed time resolution. In contrast with the multiple component output of a $BaF_2$ scintillator used in our previous study of the time evolution of pure nuclear reflections,[4] the single-component fast decay of the plastic scintillator allowed nuclear-resonant signals at times as fast as 10 nsec following the strong "prompt" electronic scattering signal to be easily observed. To reduce noise, the outputs of two phototubes viewing a single scintillator were measured in coincidence. No orienting magnetic field was applied in this experiment.

Figure 1 shows the time-dependent scattering from the (888) (Ref. 17) Bragg peak from a nearly perfect single crystal of $Fe_2O_3$. In (a) the monochromatic exciting radiation was tuned to the 14.4-keV resonance and in (b) the energy was offset by 50 meV. Both curves are dominated by a prompt peak at time zero. This signal originates from the normal charge scattering at the (888) allowed Bragg peak. On resonance there is also structure in the 5–50-nsec region which is not observed in the off-resonance data. This signal arises from resonant scattering from the $^{57}$Fe nuclei.

The experimental setup permitted varying not only the

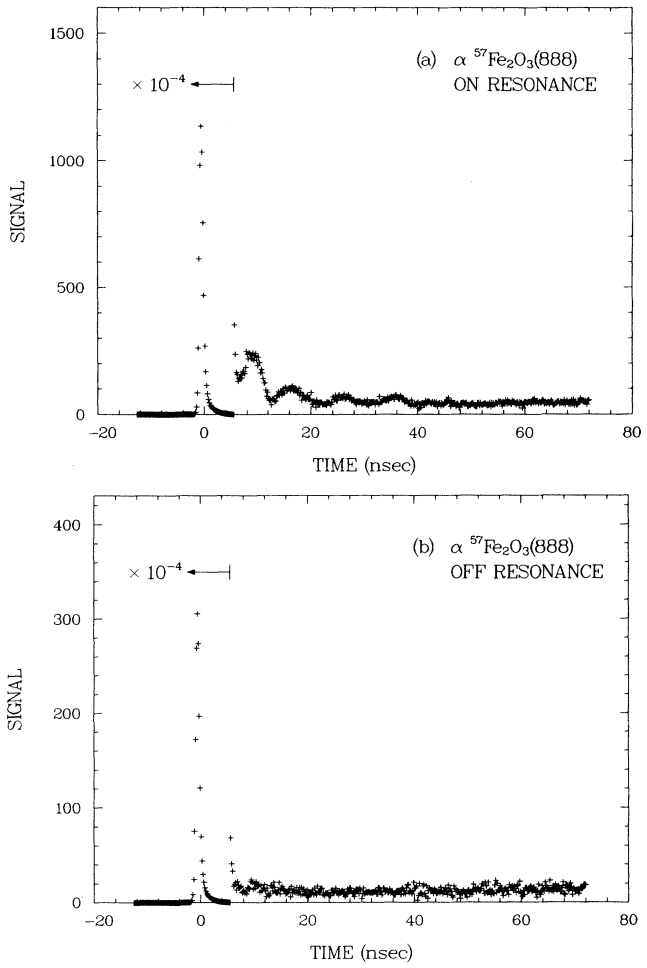


FIG. 1. Time response of the scattering from the (888) Bragg peak in $Fe_2O_3$, with (a) the probe energy set on resonance, and (b) the probe energy detuned by 50 meV. In both cases, the prompt ($t=0$) scattering has been scaled by $10^{-4}$.

Bragg angle of the $Fe_2O_3$ sample but also the energy of the exciting synchrotron beam which has an energy width of 5 meV. To verify the origin of the delayed signal (5–25 nsec) in Fig. 1(a) two further measurements were made. First, the energy of the probe beam was varied with the sample set at the Bragg angle. The variation of Bragg angle over the range of energy scanned was small compared to the rocking-curve width of the (888) reflection (3 arcsec). The results of this energy scan are shown in Fig. 2. A peak with FWHM of 5 meV is seen centered at an energy where the pure nuclear (777) Bragg peak has been observed and studied in detail previously.[3] The observed width is just the resolution of the probe beam.

A second measurement using only the delayed signal was also made. A normal rocking curve of the (888) delayed intensity was measured with the energy of the probe beam set on resonance (peak in Fig. 2) and 18.6-

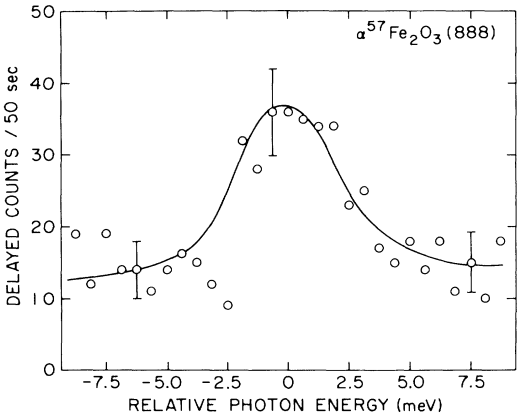


FIG. 2. Plot of delayed counts vs energy of the probe beam, referenced to the $^{57}$Fe resonance.

meV off resonance. The upper panel of Fig. 3 shows the on-resonance rocking curve. The observed profile is the same as that measured with the prompt signal arising from the normal charge scattering. The lower panel shows the same scan with the probe beam detuned from the resonance by 18.6 meV. The straight line is a fit to the data and, within statistics, no peak is observed. The data presented in Figs. 1–3 demonstrate that the origin of the delayed intensity is clearly resonant and consistent with the expected response of the scattering from $^{57}$Fe nuclei.

Finally, the time response for the (888) Bragg scattering excited by the synchrotron beam was calculated and compared with experiment. Using the expressions above, the scattering strengths for the electronic and nuclear scatterings were calculated including the anomalous scattering corrections for both iron and oxygen. Isotropic Debye-Waller factors were calculated using a Debye temperature of 660 K. The Lamb-Mössbauer factors were also calculated using this value. Values of 51.5 T for the hyperfine field, 0.12 mm/sec for the quadrupole splitting, 0.097 mm/sec for the resonance width $\Gamma$, 8.21 for the conversion coefficient $\alpha$, $I_g = \frac{1}{2}$, and $I_e = \frac{3}{2}$ were used.[18] Following Kagan and Afanes'ev,[15] the sixteen independent field amplitudes corresponding to all possible polarization states were calculated numerically for an infinitely thick crystal. Then the energy dependence of the scattered amplitudes was calculated. The range of calculation, 6 times the experimental splitting of the outermost lines in the absorption spectrum of $Fe_2O_3$, was sufficient to allow removal of a constant electronic contribution to the spectrum. The resulting nuclear component was numerically Fourier transformed to obtain the time dependence. A double-Fermi-function window was used to minimize termination effects in the transform. As a check, a Gaussian window was also tried with a $\sigma$ of approximately half of the full range of the transform, and the results were the same. Also, doubling the range of the Fourier transform resulted in changes of

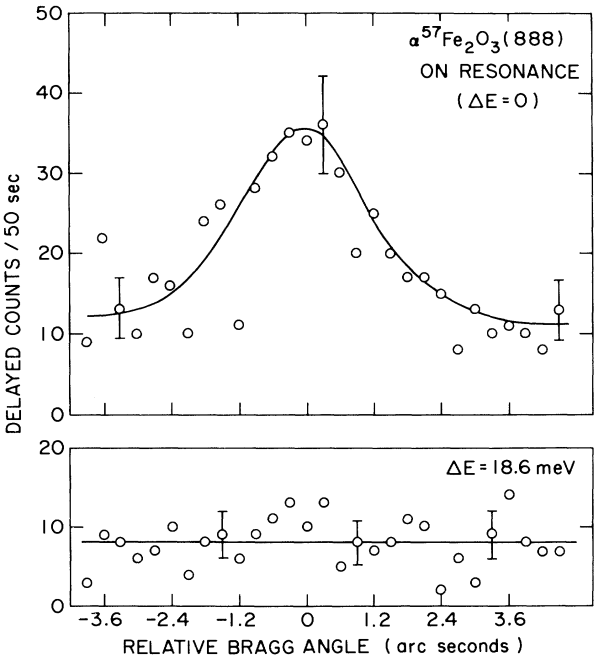


FIG. 3. Upper panel: rocking curve with the probe beam on resonance, using the delayed signal. Lower panel: probe beam detuned by 18.6 meV.

less than 10% in the overall results. Finally, the calculation was averaged over the direction of the quantization axis, and also over the exact Bragg angle to account for crystal imperfections and the incident-beam divergence (0.4 arcsec). The angular averaging was done using a Gaussian distribution. The width $2\sigma$ and centroid were adjusted to give a good fit by eye, and the calculation was normalized to the data including a constant background.

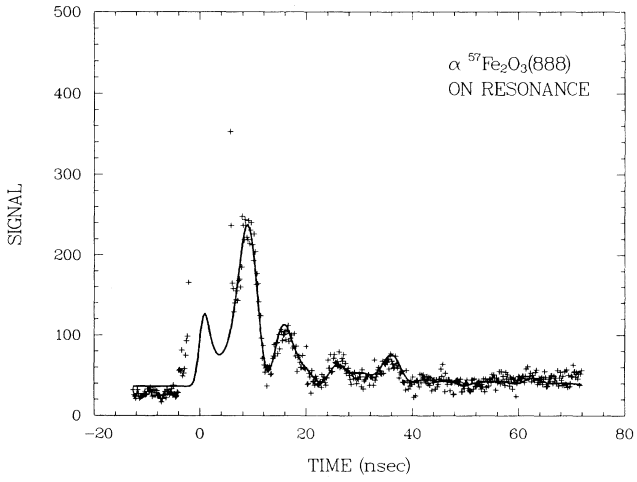


FIG. 4. Measured time dependence of the allowed (888) Bragg peak, with the prompt peak omitted. The solid line is a calculation described in the text.

The calculation, shown as the solid curve in Fig. 4, used values of 0.8 arcsec for $\sigma$ and 0.0 for the centroid shift. The experimental data shown in Fig. 4 are identical to those shown in Fig. 1(a), with the prompt peak omitted for clarity. The agreement between theory and experiment in Fig. 4 confirms the resonant nuclear origin of the delayed component of the electronically allowed Bragg reflection.

In summary, by choosing the proper experimental conditions, the delayed nuclear-resonant scattering was readily observed in the presence of strong normal charge scattering. This result paves the way for a variety of experimental studies of nuclear-resonant scattering from samples for which strong charge scattering cannot be suppressed crystallographically.

Preparation of the $^{57}Fe_2O_3$ crystal by A. Cooper and J. Remeika of AT&T Bell Laboratories is gratefully acknowledged, as is the assistance of the CHESS staff. This work was supported by the Department of Energy through Contract No. DE-AC02-76CH00016.

---

[a]Present address: Central Research Institute of Physics, Budapest, Hungary.

[1]S. L. Ruby, J. Phys. (Paris), Colloq. **35**, C6-209 (1974).

[2]A. I. Chechin, N. V. Andronova, M. V. Zelepukhin, A. N. Artem'ev, and E. P. Stepanov, Pis'ma Zh. Eksp. Teor. Fiz. **37**, 531 (1983) [JETP Lett. **37**, 633 (1983)].

[3]G. Faigel, D. P. Siddons, J. B. Hastings, P. E. Haustein, J. R. Grover, J. P. Remeika, and A. S. Cooper, Phys. Rev. Lett. **58**, 2699 (1987).

[4]G. Faigel, D. P. Siddons, J. B. Hastings, P. E. Haustein, J. R. Grover, and L. E. Berman, Phys. Rev. Lett. **61**, 2794 (1988).

[5]D. P. Siddons, J. B. Hastings, G. Faigel, L. E. Berman, P. E. Haustein, and J. R. Grover, Phys. Rev. Lett. **62**, 1384 (1989).

[6]E. Gerdau, R. Rüffer, H. Winkler, W. Tolksdorf, C. P. Klages, and J. P. Hannon, Phys. Rev. Lett. **54**, 835 (1985).

[7]E. Gerdau, R. Rüffer, R. Hollatz, and J. P. Hannon, Phys. Rev. Lett. **57**, 1141 (1986).

[8]R. Rüffer, E. Gerdau, R. Hollatz, and J. P. Hannon, Phys. Rev. Lett. **58**, 2359 (1987).

[9]U. van Bürck, R. L. Mössbauer, E. Gerdau, R. Rüffer, R. Hollatz, G. V. Smirnov, and J. P. Hannon, Phys. Rev. Lett. **59**, 355 (1987).

[10]A. N. Artem'ev, I. P. Perstnev, V. V. Sklyarevskiĭ, G. V. Smirnov, and E. P. Stepanov, Zh. Eksp. Teor. Fiz. **64**, 261 (1973) [Sov. Phys. JETP **37**, 136 (1973)]; A. N. Artem'ev, I. P. Perstnev, V. V. Sklyarevskiĭ, and E. P. Stepanov, Zh. Eksp. Teor. Fiz. **73**, 1108 (1977) [Sov. Phys. JETP **46**, 587 (1977)].

[11]D. P. Siddons, J. B. Hastings, and G. Faigel, Nucl. Instrum. Methods Phys. Res., Sect. A **266**, 329 (1988).

[12]G. T. Trammel, in *Chemical Effects of Nuclear Transformations* (IAEA, Vienna, 1961), Vol. 1, p. 75.

[13]A. M. Afanas'ev and Yu. Kagan, Zh. Eksp. Teor. Fiz. **48**, 327 (1965) [Sov. Phys. JETP **21**, 215 (1965)].

[14]J. P. Hannon and G. T. Trammell, Phys. Rev. **186**, 306 (1969).

[15]Yu. Kagan and A. M. Afanas'ev, Z. Naturforsch. **28a**, 1351 (1973).

[16]U. van Bürck, G. V. Smirnov, R. L. Mössbauer, F. Parak, annd N. A. Semioschkina, J. Phys. C **11**, 2305 (1978).

[17]All indices are referred to the rhombohedral unit cell.

[18]O. C. Kistner and A. W. Sunyar, Phys. Rev. Lett. **4**, 412 (1960).